Available online at www.eccomasproceedia.org
Eccomas Proceedia SMART (2023) 886-898

ECCOMAS
Proceedia

X ECCOMAS Thematic Conference on Smart Structures and Materials
SMART 2023
D.A. Saravanos, A. Benjeddou, N. Chrysochoidis and T. Theodosiou (Eds)

From single- to multi-stiffened panels : Upscaling a data-driven methodology for remaining useful life prediction

GEORGIOS GALANOPOULOS [*], EFTHIMIOS FYTSILIS [*], NAN YUE [†], AGNES BROER [†], DIMITRIOS MILANOSKI [*], DIMITRIOS ZAROUCHAS [†] AND THEODOROS LOUTAS [*]

[*] Department of Mechanical Engineering and Aeronautics
University of Patras
Rio University Campus, 26504 Rio, Greece

[†] Center of Excellence in Artificial Intelligence for structures
Aerospace Engineerign faculty, Delft University of Technology
Kluyverweg 1, 2629HS Delft, the Netherlands

Abstract. In this paper we propose a methodology for Remaining Useful Life (RUL) estimation of multi-stiffened composite panels utilizing the degradation data of simpler structures, i.e., single-stiffened panels. Distributed Fiber Optical sensors (DFOS) are employed to monitor the panels' behavior under multiple impact, variable amplitude compression-compression fatigue. An effective and efficient data processing methodology is first applied to the DFOS data, to both negate the effects of the variable loading conditions and ease the computational burden. For the latter, virtual FBG sensors are created from the DFOS data, in an attempt to also mimic the sensing conditions of the single-stiffened panels. In this upscaling endeavor, an advanced strain-based Health Indicator (HI) based on Genetic algorithms, created and validated on the single-stiffened panel data, is used as the prognostic feature for the RUL estimations of the multi-stiffened panels. The HI displays favorable characteristics in terms of monotonicity and prognosability which are highly desirable for more accurate RUL estimations. For this prediction task, machine learning models are trained using the historical degradation data of the single-stiffened panels and a similarity analysis is performed to enhance the accuracy when predicting the RUL of the multi-stiffened panels. Despite the increased complexity of the multi-stiffened panels, the RUL was able to be predicted with great accuracy demonstrating the benefit of the proposed methodology, from data processing to similarity RUL estimation.

Keywords: Structural Health Monitoring, Composite Structures, Stiffened panels, Compression fatigue, Remaining Useful Life prediction

1 INTRODUCTION

In the last few decades composite materials have seen an increased use in various fields of engineering with aerospace and automotive being some of the industries which are taking advantage of their unique mechanical properties. However, composite materials suffer from a

Peer-review under responsibility of the organizing committee of SMART 2023.
doi: 10.7712/150123.9841.443833

significant disadvantage; their inhomogeneous, anisotropic nature, as well as the variety of different, interacting damage mechanisms make their degradation extremely hard to comprehend and model. In service, such materials are subjected to multiple loading and environmental conditions which further complicates their degradation behavior. To this end, advance monitoring technologies need to be employed to efficiently monitor them.

Structural Health Monitoring (SHM) is an emerging concept, gaining increased attention over the past couple of decades. In the final level of SHM is prognostics, and the term Remaining Useful Life (RUL) prognosis [1], which helps estimate the imminence of failure occurring and plan required maintenance actions.

RUL prognostics; especially in composite materials; is a topic still at its infancy. The three main approaches to RUL are model-based, data-driven and hybrid approaches [2]. Model-based approaches rely on mathematical models to model the degradation and estimate the RUL, while data-driven model use condition monitoring data to build the prediction models using machine (ML) learning. Hybrid approaches refer to a combination of the previous two approaches. Several researchers has attempted to study the task of RUL prognosis though the focus has been mostly placed in machinery and systems [3]–[5], while only few study composite structures. There have been some model-based approaches for RUL estimation of composites. Stiffness degradation models [6], modified Paris law models [7], and Bayesian framework models are commonly used [8], [9]. Due to the complexity of accurately modeling the degradation of composite materials, data-driven models are usually preferred. Liu et al. [10] proposed a Gaussian Process model to predict the RUL of composite beams using damage indexes extracted from acoustic emission (AE) and PZT condition monitoring data. Eleftheroglou et al. [11] proposed a Non-Homogeneous Hidden Semi Markov Model (NHHSMM) which estimates the degradation and the RUL using strain data from open-hole composite coupons. The same model was used for RUL prediction using AE features and was compared with a Bayesian Neural Network (BNN) [12]. The NHHSMM was found to outperform the BNN, with more coherent predictions and converging confidence intervals. Galanopoulos et al. [13], proposed a degradation feature based on genetic algorithm optimization, which was used to predict the RUL of stiffened composite panels using GPR and the NHHSMM.

In a continuation of our previous research [14], we investigate the feasibility of upscaling the methodologies from single-stiffened panels (SSPs) to multi-stiffened panels (MSPs) with 5 stiffeners. Strain data collected from Distributed Fiber optical sensors (DFOS) are processed to extract useful information in the form of HIs [15], [14], which possess promising prognostic attributes. Finally, the advanced HI is used to predict the RUL of the SSPs using an ensemble learning framework trained with data from the SSPs and a predefined failure threshold.

The paper is structured as follows, section 2 describes the experimental campaign and pre-processing methodologies, section 3 presents the ensemble learning framework and the regression algorithms. Section 4 discusses the preliminary results and shows the RUL prediction, and finally, the paper is summarized in section 5.

2 EXPERIMENTAL CAMPAIGN

2.1 Specimen and experiment definition

Five-stringered composite panels were manufactured from IM7/8552 unidirectional prepreg CFRP. The layup for the skin and T-shaped stiffeners are [45/-45/0/45/90/-45/0]s and [45/-45/0/-45/45]s, respectively. Resin tabs are cast on the panels' top and bottom free edges to ensure proper load introduction and uniform loading. The panels have a length of $1100\ mm$ and the width is $850\ mm$. A schematic representation of the panel geometry is shown in Figure 1. Before subjecting the panels to fatigue tests, a quasi-static compression test with a constant displacement rate of 0.5 mm/min is performed to assess the ultimate compression strength and guide the decision of the fatigue loads. The collapse load was estimated at 310 kN and based on this result, the initial fatigue load is determined.

To create stress concentration areas, Barely Visible Impact Damage (BVID) is induced. The panels are impacted multiple times from the skin side with various energies, using an air gun, as analyzed in Table 1. The initial fatigue load was determined similar to [15], [16], around 60% of the collapse load. The variable loading conditions are created for two reasons. First, similar to [14], [15], to create different loading scenarios and evaluate the ability of our methodologies to tackle and adapt to these scenarios. Secondly, the loads were adapted to account for a snap-back effect [17], [18], in order to eliminate this behavior. The loads and fatigue life can be seen in Table 1.

The variable amplitude compression fatigue tests are performed in the Aerospace Structures and Materials Laboratory of Delft University of Technology in an MTS hydraulic machine with 14.3 tons load capacity with a constant frequency of 1 Hz and load ratio of 10.

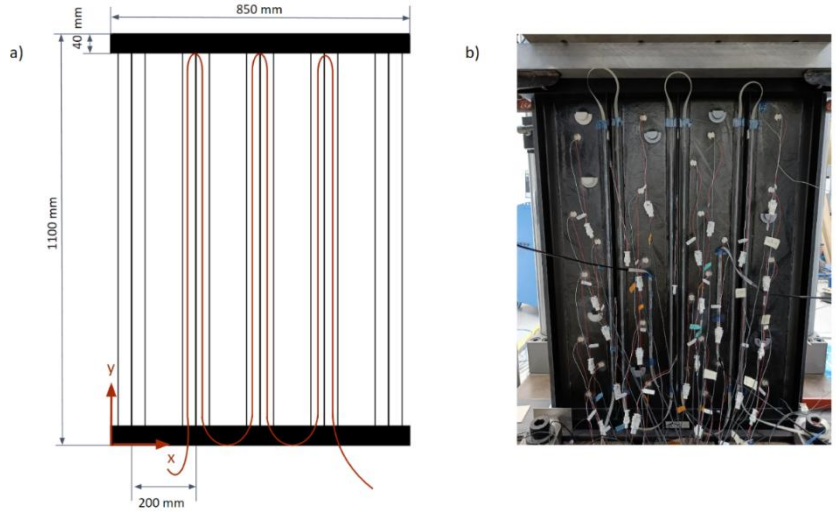

***Figure 1**: Schematic representation of the MSP and sensorised MSP on the test machine*

***Table 1**: MSP load and damage initial damage information*

Specimen #	Impact Location	Impact Energy	Max Load [kN]	# of Cycles

	[X, Y]			
MSP 01	[25.3, 79.5]	15.2 J	-195	8
	[40, 80]	19.8 J	-185	2076
	[45.5, 66]	15.2 J	-100	350 k
	[58, 64.5]	17.2 J	-150	13 k
			-120	50 k
			-200	136 k
			-230	540 k
				Total: 1046 k
MSP02	[40.5, 58]	13 J	-150	680 k
			-170	120 k
			-200	110 k
			-230	230 k
				Total: 1140 k
MSP 03	[25.5, 66.5]	15.2 J	-200	Total: 540 k
	[39.6, 66.6]	17.2 J		
	[46, 79]	15.2 J		
	[59.5, 78.9]	25.2 J		

Regarding the SHM methodologies used to monitor the fatigue behavior, the panels are equipped, among others, with a distributed fiber optic sensing (DFOS) system. The DFOS is encase in a SMARTape^{TM} [19], and is bonded with acrylic glue on both feet of the three middle stiffeners. The total measuring length is approximately $5\,m$, $840\,mm$ per foot, focused on the middle section. The LUNA odisi-B acquisition system is used with an acquisition frequency of $23.8\,Hz$ and a spatial resolution of $0.65\,mm$.

The loading sequence is depicted in Figure 2. Every 1000 cycles, fatigue is stopped and the panel is subjected to quasi-static (QS) loadings from 5 kN up to the maximum fatigue load level under a constant displacement rate of $0.5\,mm/min$, during which the DFOS measurement were obtained. Every 10000 cycles, the applied load is reduced to 5 kN to allow for LW measurements. The load is arbitrarily changed after a few tens of thousands of cycles for the aforementioned reasons.

2.2 Pre-Processing methodologies

Under the variable loading conditions (which are closer to real life operational conditions), the peak strains display a certain variability, that does not represent only damage accumulation as it is desired, but also the effect of the changing loads. Hence, it is important to discover a pre-processing methodology attempting to eliminate the effects of the varying loads. A first attempt to eliminate the variable loading effect was proposed in [15]. In this research we build on and extend our previous methodology.

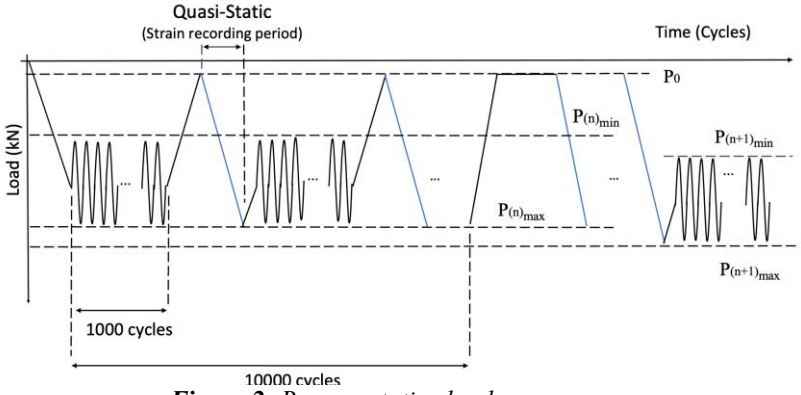

***Figure 2**: Representative load sequence*

In the first step, data are processed in the spatial domain. Since measurements are available every $0.65\ mm$ for $5\ m$, down sampling is performed and only k data points are retained per foot as virtual FBG (vFBG) sensors. Since the panels are approximately 3 time larger than the SSPs, $k = 15$ was used. The vFBGs were space equally along the measurement length with a spacing of $50\ mm$. In Figure 3a, the strain through time of a single vFBG is presented. In the time axis, to eliminate the load effect n random points of each QS are sampled, equal to 1/3 of the total sample length, using a uniform distribution (see Figure 3a) and the average of these points is considered as the strain at each time instance. The results are then smoothed via a moving average filter (Figure 3b).

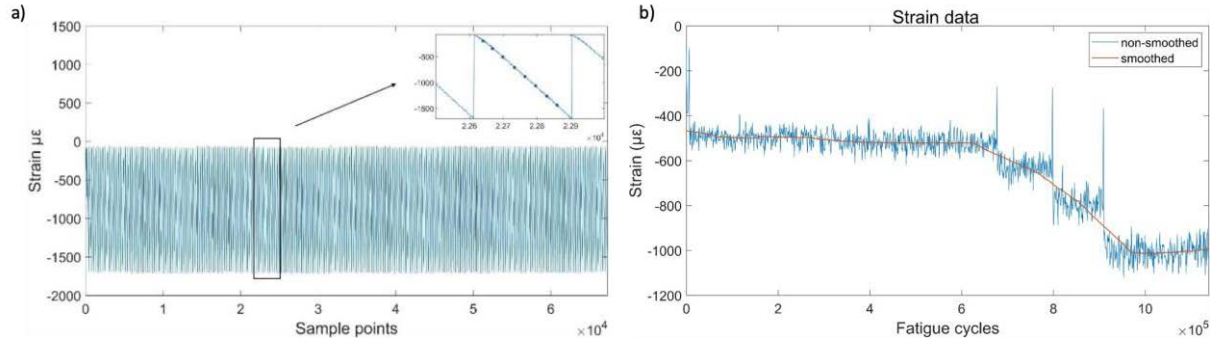

***Figure 3**: Pre-processing methodology in the time axis. a) figure represent the quasistatic through time for a vFBG and b) figure the final extracted unsmoothed and smoothed strain.*

3 METHODOLOGIES

An ensemble learning similarity framework is proposed to tackle the challenging task of RUL estimation.

3.1 Ensemble learning

Ensemble learning entails training diverse sub-models and using their combined outputs for extrapolating the final results. A proper weighting strategy can enhance the ensemble results. Bauer et al. [20] has shown that such models are able to provide superior performance by taking advantage of the diverse outputs of each model. A typical ensemble model can be

seen in Figure 5. Diverse sub-models using the database of available SSPs are built. This option provides not only a variety of different failure scenarios and lifetimes, but also variety of different loading conditions and initial damages.

3.2 Similarity Analysis

The To effectively exploit the output of the diverse sub-models an efficient dynamic-weighting strategy is implemented. Similar to [21] a Fuzzy Similarity Analysis (FSA) scheme is proposed, to calculate dynamic, time varying weights for each sub-model. More specifically, we aim to estimate the similarity between each MSP's degradation curve, represented by HI, with each SSP's from the available historic database. In total there are $M = 15$ available degradation instances of HI_{GA} comprising our database.

Let $D = (d_1, d_2, \dots, d_N)$ be the degradation trend of a j[th] SSP and $x = (x_1, x_2, \dots, x_L)$ the degradation curve of the MSP, where $L \neq N$ the different sequence lengths. Then the weights for each sub-model are calculated as follows:

1. *Pointwise Euclidean distance computation.* The first step consists of calculating the Euclidean distance between D and x denoted with the vector $\delta_{i\times 1} = \|D - x\|^2$ for $i = \ , \dots, min\ (N, L)$.

2. *Pointwise distance scoring.* Triangular, trapezoidal, and bell-shaped are among the most popular functions for similarity scoring [22]. In this work, a bell-shaped function shown in Eq. (1) is used, since it provides more robust results due to its gradual smoothness:

$$\mu_{i\times 1} = exp\ (-(\frac{-ln\ (\alpha)}{\beta^2})\delta_{i\times 1}) \quad (1)$$

Where α and β are parameters which define the shape of the similarity measure to the fuzzy rule set. Through trial and error, $\alpha = 5.75$ and $\beta = 0.5$ are used. For SSPs with shorter sequence lengths (shorter lifetime) are set to 0 after failure has occurred. The distance score $d_l = \ - \mu_l$ is computed, where $l = 1, \dots, L$.

3. *Weight definition.* Finally, the weight w_l given to the jth training specimen, accounting for how similar it is to the test one, is computed by the arbitrarily chosen decreasing monotone function, which guarantees that the smaller the distance d_l the larger the impact given to the jth specimen.

$$w_l = (1 - d_l) \cdot exp\ (-\frac{}{\beta} d_l) \quad (2)$$

By repeating the previous steps for all available sub-models, the weight matrix $W_{L\times M}$ is obtained. These weights are applied in the ensemble learning paradigm to derive the final output of the ensemble model for each MSP. Given HI_{GA} of one MSP as the input vector x to

the prognostic sub-models created, from each SSP, the predicted value of its RUL using the subsequent $j = 1, \dots, N$ sub-model is represented as $\hat{y}_j = f(x)$, where $f(\cdot)$ is the regression approach.

Then, the proposed simple but efficient strategy for combining sub-model outputs is to estimate the RUL as a weighted mean of those N sub-models:

$$\hat{y} = \frac{}{M} \sum_{j=1}^{M} w_j \cdot \hat{y}_j \quad (3)$$

3.3 Regression Algorithms

LSTM Network

The Long Short-Term Memory (LSTM) neural network, which belongs to the Recurrent Neural Network (RNN) family, was initially described in [23]. Unlike traditional RNNs, LSTM includes a memory cell that assesses whether past information is still relevant or not, preventing the vanishing or exploding gradient problem when processing long sequences. Consequently, it maintains a steady error that can be back propagated through time and layers, allowing the network to learn continuously over extended periods [24]. LSTM's fundamental principle is that its memory cell serves as a repository of state information, functioning like a conveyor belt that runs through the entire chain with only minor linear interactions. The information flows effortlessly and remains unchanged. Gates, such as the forget gate, the input gate, and the output gate, are used in LSTM to remove or add information to the cell state. Our proposed LSTMN architecture can be seen in Figure 4. The network comprises of the input layer, the LSTM layer, the fully connected layer, a dropout layer and finally, the regression output layer. The input layer accepts as input a time series data string, while dependences between input and targets are learned at the LSTM layer. Dropout layer serves as guard against overfitting and improving the generalization capabilities. For the training of the LSTM network, since it is prone to the scale of the data, a normalization methodology is employed according to:

$$y' = \frac{y - y_{min}}{y_{max} - y_{min}} \quad (11)$$

Consequently, the model learns to predict the RUL in the $[0,1]$ range as a percentage rather than as the anticipated cycles.

Training is conducted for 100 epochs utilizing the Adam algorithm. For simplicity, the final model, which is universally used for all SSPs, has a LSTM layer with 64 hidden units, a dropout probability $p = 0.2$ and lastly the regression layer of size 1 is used to minimize the half-mean-squared-error (MSE) of the predicted responses for each time step as the loss function:

$$MSE = \frac{}{2M} \sum_{l=1}^{M} (y_l - \hat{y}_l)^2 \quad (12)$$

M is the sequence length. For uncertainty quantification, the bootsrap algorithm [25] is used.

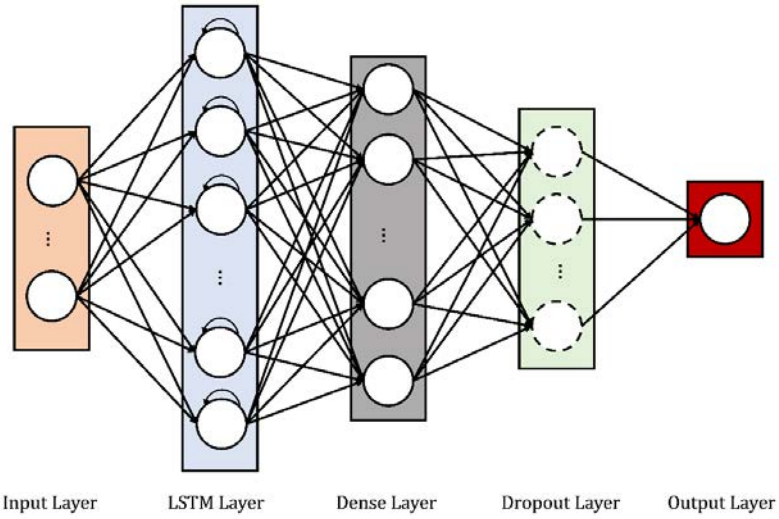

***Figure 4**: Proposed LSTMN network architecture*

Gaussian Process Regression

Gaussian processes (GPs) have been previously employed in predicting the RUL of a structures [10], [26]. GPs constitute of a set of random variables following a joint Gaussian distribution, and are a function of $f(\boldsymbol{x})$ at $\boldsymbol{x}= [x_1, x_2, \ldots, x_n]^T$. GP can be defined [27] by its mean function $m(x) = E[f(x)]$ and covariance function $k(x, x') = E[(f(x) - m(x))(f(x') - m(x'))]$. Then the GP is expressed as $f(x) \sim GP(m(x), k(x, x'))$.

Typically, the mean function $m(x)$ is chosen to be zero, but in our case, we opted for a linear function $m(x) = ax + b$. As noted in [27] different covariance functions yield different regression results, so the selection of this function should be done with caution based on the data. It was observed that our data are better represented by a Mattern 5/2 covariance function:

$$k(r) = \sigma_f^2 \left(1 + \frac{\sqrt{5}r^2}{\sigma_l^2} + \frac{5r^2}{3\sigma_l^2}\right) exp\ exp\ \left(-\frac{\sqrt{5}r}{\sigma_l}\right) \quad (13)$$

Let x_i represent the input variables, and $y_i = f(x_i) + \varepsilon_i$ represents the noisy target variables, with ε_i being an i.i.d with mean 0 and variance σ_n^2. The joint distribution of observed target values $y = [y_i]_{i=1}^N$ and unobserved target values f^* at new input locations x^* can be denoted as:

$$[y\ f^*] \sim N\ (0, [K(x,x) + \sigma_n^2 I\ K(x,x^*)\ K(x^*,x)\ K(x^*,x^*)]) \quad (14)$$

I is the identity matrix and K a matric containing the covariance pairs of x and x^*. The posterior distribution for GPR, given the new inputs x^*, the historic input data x and targets y is defined by:

$$p(x, y, x^*) \sim N\left(\underline{f^*}, cov(f^*)\right) \quad (15)$$

$$\underline{f}^* = E[x, y, x^*] = K(x^*, x)[K(x, x) + \sigma_n^2 I]^{-1} y, \quad (16)$$

$$cov(f^*) = K(x^*, x^*) - K(x^*, x)[K(x, x) + \sigma_n^2 I]^{-1} K(x, x^*) \quad (17)$$

4 RESULTS AND DISCUSSION

4.1 Degradation Feature

A capable degradation feature is important and can affect the accuracy of the RUL prediction. Through investigation in our previous work [14], an enhanced strain-based degradation feature was discovered using genetic algorithms.

Although the feature was discovered to have high prognosability and alleviate the need for a predefined failure threshold, due to the dissimilarity of both the testing specimens as well as the collected data, a conservative failure threshold is set at 0.84. This value is not arbitrary and corresponds to the lowest observed value of the SSP specimens at the time of failure which are used to train the predictive algorithms. The progression of HI through time for the MSPs can be seen in Figure 5. It is evident, that the behavior of the HI especially at the final stages is not desirable for two out of the three panels. An almost constant value of 1 is observed. This is a result of the raw strains displaying a constant value after a point as can be seen in our representative extracted strains (Figure 3). The normalization parameters for vHI_1 [15], are obtained through similarity analysis between the MSP and the SSPs in the first 30000 cycles.

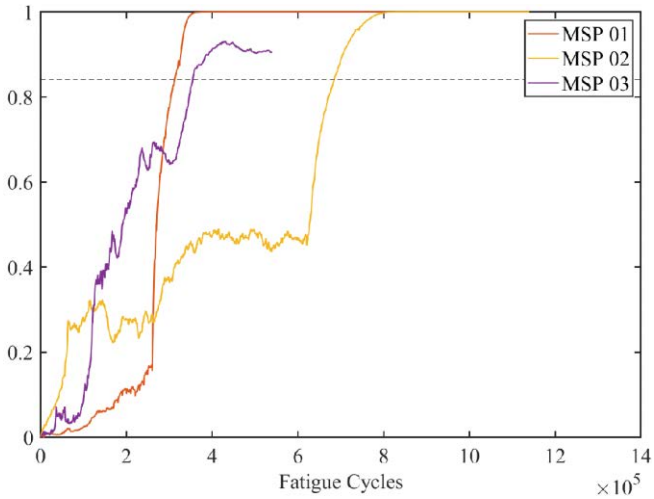

***Figure 5**: HI_{GA} progression through time for the different MSPs*

4.2 RUL prediction

An ensemble learning framework is proposed to tackle the challenging task of RUL estimation. Two distinct regression algorithms are used, LSTMN and GPR, and their predictions are compared and discussed. Both algorithms are trained using each unique SSP and their predictive outputs are combined via a dynamically weighted average, as described in Methodologies, which enhances the prognostic performance. The predicted normalized RULs and 90% confidence intervals are shown in Figure 6. It is evident that the overall RUL estimations for MSP 02 are not very good. More specifically, the predicted RUL underestimates the true one, giving conservative predictions. However, what can be seen is that both algorithms manage to converge to the true RUL near the EoL. For MSP 01 and MSP 03, RUL estimations are closer to the true RUL with the LSTMN predictions being slightly better. However, GPR edges in the estimations near the EoL which are almost similar to the true RUL. As far as the CI are concerned, for MSP 02 CI include the true RUL only at the early and later prediction stages with either algorithm. For MSP 01 and MSP 03 CIs of the LSTMN include the true RUL for most of the lifetime, though GPR only manages to include it near the EoL.

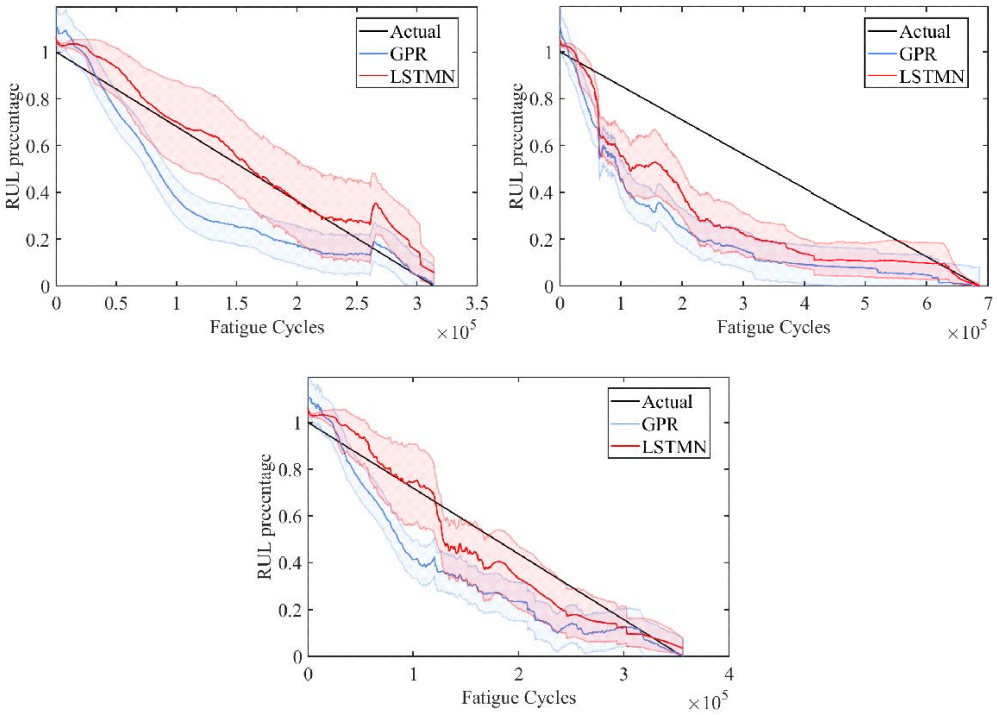

***Figure 6**: RUL estimations for the different MSPs*

To validate the qualitative observations regarding the RUL predictions some common prediction performance metrics are employed. MAPE (Mean Absolute Percentage error) and CRA (Cumulative Relative Accuracy) are preferred since they calculate the percentage and relative differences from the true RUL and can better describe our case where the calculated

RULs are in the range of [0, 1]. It can be seen, that except for MSP 02, the algorithms produce very similar results, with overall LSTM outperforming the GPR by a slight margin of less than 10%.

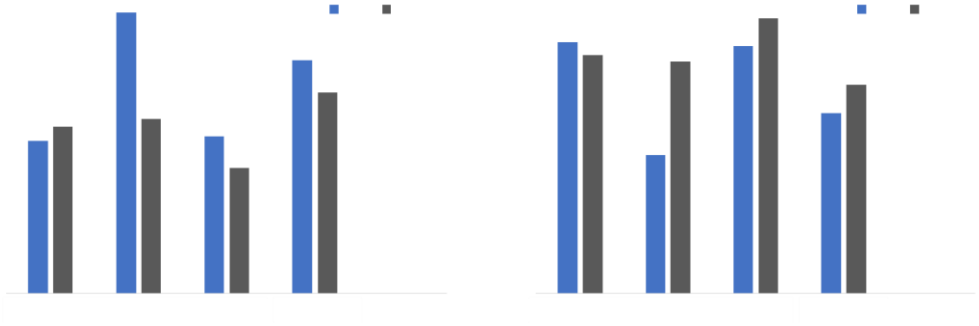

***Figure 7**: MAPE and CRA for the different MSPs*

5 CONCLUSIONS

In this paper we presented an upscaling methodology for Remaining Useful Life (RUL) estimation of multi-Stiffened composite Panels (MSPs) using data and methodologies tested and validated on Single-Stiffened composite Panels (SSPs). Novel compression-compression fatigue experiments with variable amplitude are conducted on MSP where Distributed Fiber Optical Sensors (DFOS) are employed to monitor their strain distribution along the stiffener feet. The strain data are pre-processed in two axes, the spatial and the time, where in the first a data reduction methodology is proposed and in the second an attempt to eliminate the effect of the shifting loads is made. Health Indicators (HIs) proposed in our previous work is constructed to estimate the RUL using a failure threshold based on the data from the SSP. Two machine learning algorithms are employed, Long-Short Term Memory Networks (LSTMN) and Gaussian process regression (GPR) for RUL prediction. An ensemble learning similarity framework is proposed, which trains unique models using the SSP specimens and then combines their output using a similarity weighted mean. Confidence intervals (CIs) are an inherent property of the GPR, however, for the LSTMN, the bootsrap algorithm is used to create them. The estimated RUL shows good results, managing to stay close to the true RUL especially near the End of Life (EoL) which is a result of the predefined failure threshold. What is observed, is that the quality of the HI greatly affects the predicted RUL and that more gradual behavior leads to better overall estimations. The major setback of the proposed methodology lies with the arbitrary EoL threshold. For this threshold to be more robust and meaningful, correlation with a degradation property such as damage size or stiffness reduction is necessary. Overall, this first attempt of upscaling the previously developed methodologies is considered successful.

REFERENCES

[1] A. Saxena, K. Goebel, C. C. Larrosa, V. Janapati, S. Roy, and F.-K. Chang, “Accelerated Aging Experiments for Prognostics of Damage Growth in Composite

Materials." Sep. 01, 2011, Accessed: Feb. 16, 2022. [Online]. Available: https://apps.dtic.mil/sti/citations/ADA584693.

[2] J. Guo, Z. Li, and M. Li, "A Review on Prognostics Methods for Engineering Systems," *IEEE Trans. Reliab.*, vol. 69, no. 3, pp. 1110–1129, Sep. 2020, doi: 10.1109/TR.2019.2957965.

[3] J. Z. Sikorska, M. Hodkiewicz, and L. Ma, "Prognostic modelling options for remaining useful life estimation by industry," *Mech. Syst. Signal Process.*, vol. 25, no. 5, pp. 1803–1836, 2011, doi: 10.1016/j.ymssp.2010.11.018.

[4] X.-S. Si, W. Wang, C.-H. Hu, and D.-H. Zhou, "Remaining useful life estimation – A review on the statistical data driven approaches," *Eur. J. Oper. Res.*, vol. 213, no. 1, pp. 1–14, 2011, doi: 10.1016/j.ejor.2010.11.018.

[5] Y. Lei, N. Li, L. Guo, N. Li, T. Yan, and J. Lin, "Machinery health prognostics: A systematic review from data acquisition to RUL prediction," *Mech. Syst. Signal Process.*, vol. 104, pp. 799–834, 2018.

[6] T. Peng, Y. Liu, A. Saxena, and K. Goebel, "In-situ fatigue life prognosis for composite laminates based on stiffness degradation," *Compos. Struct.*, vol. 132, pp. 155–165, 2015, doi: 10.1016/j.compstruct.2015.05.006.

[7] C. Tao, H. Ji, J. Qiu, C. Zhang, Z. Wang, and W. Yao, "Characterization of fatigue damages in composite laminates using Lamb wave velocity and prediction of residual life," *Compos. Struct.*, vol. 166, pp. 219–228, 2017, doi: 10.1016/j.compstruct.2017.01.034.

[8] M. Corbetta, A. Saxena, M. Giglio, and K. Goebel, "Evaluation of multiple damage-mode models for prognostics of carbon fiber-reinforced polymers," *Struct. Heal. Monit. 2015 Syst. Reliab. Verif. Implement. - Proc. 10th Int. Work. Struct. Heal. Monit. IWSHM 2015*, vol. 2, pp. 609–616, 2015, doi: 10.12783/SHM2015/78.

[9] M. Corbetta, C. Sbarufatti, M. Giglio, A. Saxena, and K. Goebel, "A Bayesian framework for fatigue life prediction of composite laminates under co-existing matrix cracks and delamination," *Compos. Struct.*, vol. 187, pp. 58–70, Mar. 2018, doi: 10.1016/J.COMPSTRUCT.2017.12.035.

[10] Y. Liu, S. Mohanty, and A. Chattopadhyay, "A Gaussian process based prognostics framework for composite structures," in *Modeling, Signal Processing, and Control for Smart Structures 2009*, 2009, vol. 7286, p. 72860J.

[11] N. Eleftheroglou and T. Loutas, "Fatigue damage diagnostics and prognostics of composites utilizing structural health monitoring data and stochastic processes," *Struct. Heal. Monit.*, vol. 15, no. 4, pp. 473–488, 2016.

[12] T. Loutas, N. Eleftheroglou, and D. Zarouchas, "A data-driven probabilistic framework towards the in-situ prognostics of fatigue life of composites based on acoustic emission data," *Compos. Struct.*, vol. 161, pp. 522–529, 2017, doi: 10.1016/j.compstruct.2016.10.109.

[13] G. Galanopoulos, N. Eleftheroglou, D. Milanoski, A. Broer, D. Zarouchas, and T. Loutas, "An SHM Data-Driven Methodology for the Remaining Useful Life Prognosis of Aeronautical Subcomponents," in *Lecture Notes in Civil Engineering*, 2023, vol. 253 LNCE, pp. 244–253, doi: 10.1007/978-3-031-07254-3_24.

[14] G. Galanopoulos, N. Eleftheroglou, D. Milanoski, A. Broer, D. Zarouchas, and T. Loutas, "A novel strain-based health indicator for the remaining useful life estimation of degrading composite structures," *Compos. Struct.*, vol. 306, p. 116579, Feb. 2023, doi: 10.1016/J.COMPSTRUCT.2022.116579.

[15] G. Galanopoulos, D. Milanoski, A. Broer, D. Zarouchas, and T. Loutas, "Health monitoring of aerospace structures utilizing novel health indicators extracted from complex strain and acoustic emission data," *Sensors*, vol. 21, no. 17, p. 5701, 2021.

[16] A. Broer, G. Galanopoulos, R. Benedictus, T. Loutas, and D. Zarouchas, "Fusion-based damage diagnostics for stiffened composite panels," *Struct. Heal. Monit.*, p. 14759217211007128, 2021.

[17] M. Stein, *The phenomenon of change in buckle pattern in elastic structures*. 1959.

[18] B. G. Falzon and M. Cerini, "An automated hybrid procedure for capturing mode-jumping in postbuckling composite stiffened structures," *Compos. Struct.*, vol. 73, no. 2, pp. 186–195, May 2006, doi: 10.1016/J.COMPSTRUCT.2005.11.053.

[19] D. Inaudi and B. Glisic, "Development of distributed strain and temperature sensing cables," in *17th International Conference on Optical Fibre Sensors*, 2005, vol. 5855, pp. 222–225.

[20] E. Bauer and R. Kohavi, "Empirical comparison of voting classification algorithms: bagging, boosting, and variants," *Mach. Learn.*, vol. 36, no. 1, pp. 105–139, 1999, doi: 10.1023/A:1007515423169/METRICS.

[21] J. Liu, V. Vitelli, E. Zio, and R. Seraoui, "A Novel Dynamic-Weighted Probabilistic Support Vector Regression-Based Ensemble for Prognostics of Time Series Data," *IEEE Trans. Reliab.*, vol. 64, no. 4, pp. 1203–1213, Dec. 2015, doi: 10.1109/TR.2015.2427156.

[22] F. Di Maio and E. Zio, "Failure prognostics by a data-driven similarity-based approach," *Int. J. Reliab. Qual. Saf. Eng.*, vol. 20, no. 1, Mar. 2013, doi: 10.1142/S0218539313500010.

[23] S. Hochreiter and J. Schmidhuber, "Long Short-Term Memory," *Neural Comput.*, vol. 9, no. 8, pp. 1735–1780, Nov. 1997, doi: 10.1162/NECO.1997.9.8.1735.

[24] S. Bouktif, A. Fiaz, A. Ouni, and M. A. Serhani, "Optimal Deep Learning LSTM Model for Electric Load Forecasting using Feature Selection and Genetic Algorithm: Comparison with Machine Learning Approaches †," *Energies 2018, Vol. 11, Page 1636*, vol. 11, no. 7, p. 1636, Jun. 2018, doi: 10.3390/EN11071636.

[25] A. Khosravi, S. Nahavandi, … D. C.-I. T. on, and undefined 2011, "Comprehensive review of neural network-based prediction intervals and new advances," *ieeexplore.ieee.org*, Accessed: Sep. 22, 2022. [Online]. Available: https://ieeexplore.ieee.org/abstract/document/5966350/.

[26] Y. Liu, S. Mohanty, and A. Chattopadhyay, "Condition Based Structural Health Monitoring and Prognosis of Composite Structures under Uniaxial and Biaxial Loading," *J. Nondestruct. Eval.*, vol. 29, no. 3, pp. 181–188, 2010, doi: 10.1007/s10921-010-0076-2.

[27] C. K. Williams and C. E. Rasmussen, *Gaussian processes for machine learning*, vol. 2, no. 3. MIT press Cambridge, MA, 2006.